entropy

MDPI

Article

Nano-Crystallization of High-Entropy Amorphous $NbTiAlSiW_xN_y$ Films Prepared by Magnetron Sputtering

Wenjie Sheng [1], Xiao Yang [1,2], Cong Wang [3] and Yong Zhang [1,*]

1 State Key Laboratory for Advanced Metals and Materials, University of Science and Technology Beijing, Xueyuan Road 30#, Beijing 100083, China; shengwj999@163.com (W.S.); yangxiao_sky@163.com (X.Y.)
2 State Key Laboratory of Advanced Metallurgy, University of Science and Technology Beijing, Beijing 100083, China
3 Center for Condensed Matter and Materials Physics, Department of Physics, Beihang University, Beijing 100191, China; congwang@buaa.edu.cn
* Correspondence: drzhangy@ustb.edu.cn; Tel.: +86-10-6233-3073

Academic Editor: An-Chou Yeh
Received: 30 April 2016; Accepted: 6 June 2016; Published: 13 June 2016

Abstract: High-entropy amorphous $NbTiAlSiW_xN_y$ films (x = 0 or 1, *i.e.*, $NbTiAlSiN_y$ and $NbTiAlSiWN_y$) were prepared by magnetron sputtering method in the atmosphere of a mixture of N_2 + Ar (N_2 + Ar = 24 standard cubic centimeter per minute (sccm)), where N_2 = 0, 4, and 8 sccm). All the as-deposited films present amorphous structures, which remain stable at 700 °C for over 24 h. After heat treatment at 1000 °C the films began to crystalize, and while the $NbTiAlSiN_y$ films (N_2 = 4, 8 sccm) exhibit a face-centered cubic (FCC) structure, the NbTiAlSiW metallic films show a body-centered cubic (BCC) structure and then transit into a FCC structure composed of nanoscaled particles with increasing nitrogen flow rate. The hardness and modulus of the as-deposited $NbTiAlSiN_y$ films reach maximum values of 20.5 GPa and 206.8 GPa, respectively. For the as-deposited $NbTiAlSiWN_y$ films, both modulus and hardness increased to maximum values of 13.6 GPa and 154.4 GPa, respectively, and then decrease as the N_2 flow rate is increased. Both films could be potential candidates for protective coatings at high temperature.

Keywords: high-entropy film; sputtering; nano-scaled particles; phase stability

1. Introduction

High-entropy alloys (HEAs), first defined by Yeh, differ from conventional alloys by containing multiple principal elements in equimolar or near equimolar ratios in the range of 5 at.%–35 at.% [1–6]. They tend to form simple BCC or FCC solid solutions, or amorphous phase and nanosized grain-containing crystalline phases. In recent years, great efforts have been focused on HEA films prepared by the magnetron sputtering method, such as, $TiVCrAlZrN_x$ [7], (TiVCrZrHf)N [8], (AlCrMoTaTi)N [9], FeCoNiCuVZrAl [10], *etc.* It has been shown that these HEA films display many advantages in terms of both mechanical and physical properties, high hardness and wear resistance [11–13], high resistance to corrosion [14], and oxidation [15], and excellent thermal stability especially when used as diffusion barriers in copper metallization [16–19]. It is well-known that transition metal nitride coatings usually show high hardness, good thermal stability, and excellent wear resistance properties, which make them widely used as protective coatings in mechanical cutting tools at high temperatures. Aiming to obtain a new type of proactive coatings for use at elevated temperatures, in this work HEA and HEA nitride films, namely $NbTiAlSiWN_y$, were deposited by direct-current (DC) reactive sputtering with a single target made of NbTiAlSiW HEA in a mixture atmosphere (N_2 + Ar). We have previously reported the microstructures and properties of $NbTiAlSiN_y$

HEA films [20]. Herein, it was thought that the addition of W might improve the thermal stability and reduce the cost. Moreover, the composition, structure, thermal stability, hardness and modulus of the $NbTiAlSiWN_x$ films are discussed in the present work.

2. Experiment Details

High-entropy films of $NbTiAlSiN_x$ and $NbTiAlSiWN_x$ were deposited on quartz glasses substrates by a reactive high vacuum DC sputtering method (SKY Technology Development Co., Ltd. Chinese Academy of Science, Shenyang, China). The targets were prepared by powder metallurgy with high purity (>99.99%) raw materials of niobium, titanium, aluminum, silicon and tungsten. All of the substrates were ultrasonically cleaned and rinsed with acetone, ethanol and deionized water for 15 min each before putting them in the vacuum chamber. High purity argon was added into the vacuum chamber when the base pressure was better than 2.0×10^{-3} Pa. The targets were cleaned by argon ion bombardment for at least for 15 min to remove any oxide or contaminants on the surface. The films were deposited in a mixture atmosphere of Ar and N_2 at room temperature with a working distance of 60 mm, and the total flow of argon and nitrogen flow rate were fixed at 24 standard cubic centimeters per minute (sccm). The working pressure was controlled at 0.6 Pa. A macro-photograph of the deposited thin films of different colors is shown in Figure 1. Because the films varied in thickness, and the color is sensitive to this property, commonly, the thicker films displayed darker colorations, while the addition of nitrogen produced lighter colored films. The structures of the films were identified by X-ray diffraction (XRD) on a Dmax diffractometer (Siemens, Berlin, Germany) using Cu $K\alpha$ (40 kV, 20 mA radiation. Microstructures of the top-view and cross-section of the as-deposited films were characterized using a scanning electron microscopy (SEM) system (Auriga Field Emission Scanning Electron Microscope, Carl Zeiss, Jena, Germany) equipped with an energy dispersive X-ray spectrometer (EDS) operated at 10 kV. The hardness and modulus of the as-deposited films were tested at five points of each sample with a nano-indenter with a Berkovich triangular pyramid indenter, and the maximum displacement into the sample surface was 200 nm. The thermal stability of the films was studied by using annealing heat treatments at a predetermined temperature.

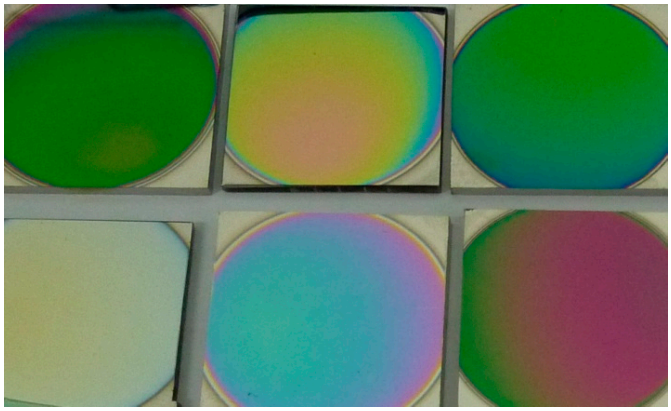

Figure 1. The macro-photograph of the deposited thin films of different colors.

3. Results and Discussion

3.1. Chemical Composition

The microstructures and properties of $NbTiAlSiN_y$ films have been presented in our previous study. The as-deposited $NbTiAlSiN_y$ films have an amorphous structure which remains stable even after exposure to a temperature of 700 °C for 24 h [20]. In this paper mainly the microstructures and mechanical properties of $NbTiAlSiWN_y$ films are discussed.

The chemical compositions of the as-deposited NbTiAlSiW metallic films with a deviation of ±0.5% are listed in Table 1. The content of nitrogen is so small that it cannot be identified by EDS. Interestingly, the compositions of the NbTiAlSiW metallic films are approximately equal to the nominal at.% values and more uniform than NbTiAlSi metallic film in depth, so near equi-atomic ratio high-entropy NbTiAlSiW metallic films are achieved.

Table 1. Compositions of the as-deposited NbTiAlSiW metallic films.

Element (at.%)	Nb	Ti	Al	Si	W
Nominal (target)	20	20	20	20	20
Actual (film) (deviation = ±0.5%)	19.8	21.1	20.2	20.5	18.4

3.2. Structure and Thermal Stability

XRD patterns of the $NbTiAlSiWN_y$ films before and after heat-treatment at 700 °C for 24 h and 1000 °C for 1 h are shown in Figure 2. For all of the as-deposited $NbTiAlSiWN_y$ films produced using various N_2 flow rates, it is clear that only one broad peak exists. This indicates the as-deposited $NbTiAlSiWN_y$ films have an amorphous structure.

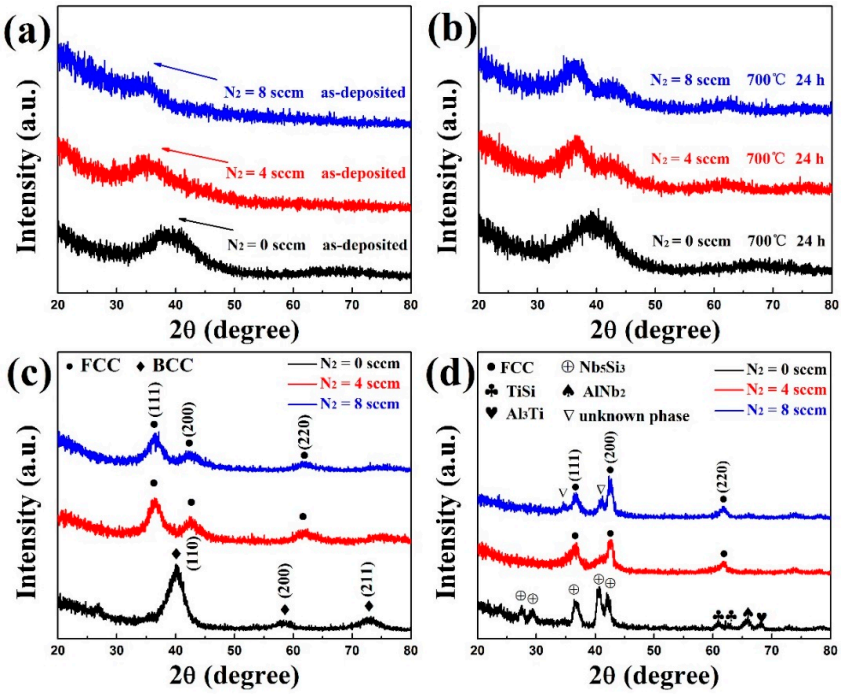

Figure 2. XRD patterns of $NbTiAlSiWN_x$ film before and after heat-treatment: (**a**) as-deposited; (**b**) 700 °C for 24 h; (**c**) 1000 °C for 1 h; (**d**) XRD patterns of $NbTiAlSiN_x$ film after heat-treatment at 1000 °C for 1 h.

Sluggish diffusion effects, high mixing entropy, and severe lattice distortions all contribute to the formation of an amorphous structure. Generally, the large atomic size differences cause severe lattice distortions and the incorporation of nitride atoms reduces the growth rate of crystallites. The rapid cooling rate during the sputtering process also plays a vitally important role in the amorphous structure formation tendency, and there is insufficient time and energy for crystallization. Additionally, the diffraction peak is shifted to lower angles and the intensity decreases with the increase of N_2 flow rate (denoted by arrows). It is proposed that the addition of nitride atoms expands the atomic space. This common phenomenon is in agreement with the results of our previous studies on $NbTiAlSiN_y$

films. Moreover, no big changes are observed after heat-treatment at 700 °C for 24 h (Figure 2b), which indicates that the $NbTiAlSiWN_y$ films still exhibit excellent thermal stability even at 700 °C. It seems to be that N atoms have almost no obvious effect on the amorphous structure when the temperature is below 700 °C. However, after heat treatment at 1000 °C for 1 h, both the $NbTiAlSiN_y$ and $NbTiAlSiWN_y$ films crystallize as nanoscale particles. After the heat treatment at 1000 °C, the NbTiAlSiW metallic film transforms from an amorphous form into a crystallized BCC solid solution structure. This change is due to the fact W and Nb have BCC structures which account for a great proportion of the weight of the film, so the BCC structure plays a dominant role without any N_2 flow, but with increasing nitrogen flow rate, the nitride films show a FCC solid solution structure with (110) preferred orientation. NbN and TiN all show FCC structures, so it is reasonable to assume that the FCC structure dominates in the crystal structure of $NbTiAlSiN_y$ nitride films. The lattice constant, atomic radius, and structures of the elements (Nb, Ti, Al and Si) and their nitrides are shown in Table 2. Both the NbTiAlSiNy and $NbTiAlSiWN_y$ system films display good thermal stability until 700 °C, but the undergo a change from an amorphous to a crystal structure after annealing at 1000 °C, with some differences in the crystallization structures.

Table 2. The lattice constants, atomic radii, and structures of each element (Nb, Ti, and Al) and nitrides.

	Nb	Ti	Al	W	NbN	TiN	AlN
Lattice constant (Å)	3.371	a = 2.950; c = 4.686	4.050	3.158	4.40	4.24	4.04
Atomic radius (Å) [21]	1.429	1.462	1.432	1.3367	-	-	-
Structure	BCC	HCP	FCC	BCC	FCC	FCC	HCP

Figure 2d shows the XRD patterns of $NbTiAlSiN_y$ films after heat treatment at 1000 °C. The NbTiAlSi metallic film forms an intermetallic structure with Nb_5Si_3, TiSi, and Al_3Ti. This is mainly due to the extremely negative mixing enthalpy between Al, Si and the other two elements (Ti and Nb). Moreover, the $NbTiAlSiN_y$ nitride films still form a FCC solid solution structure which is consistent with the results of $NbTiAlSiWN_y$ films, but when the N_2 flow rate is increased to 8 sccm, the $NbTiAlSiN_y$ films have a simple FCC solid solution structure and a small amount of an unknown phase, which requires further research, such as TEM experiments.

SEM micrographs of $NbTiAlSiN_y$ nitride films after heat treatment at 1000 °C for 1 h are shown in Figure 3. The films crystallize in nano-sized grains and the average grain size of the films deposited at 4 sccm and 8 sccm N_2 flow rate are approximately to 20 nm and 50 nm, respectively. Figure 4 shows the SEM cross-section micrographs of $NbTiAlSiWN_y$ after heat treatment at 1000 °C for 1 h. The films show a smooth cross-section without notable contrast and almost no grains can been seen at first sight. However, from the XRD pattern width at half-maximum-height, the average grain size can be calculated by Scherrer's formula [22]. With increasing N_2 flow rate, the average grain sizes of $NbTiAlSiWN_y$ films are 3.5 nm, 4.6 nm, and 5.2 nm, respectively. The films have small crystallite sizes, dense structures, and smooth surfaces, which cannot be clearly analysed by SEM.

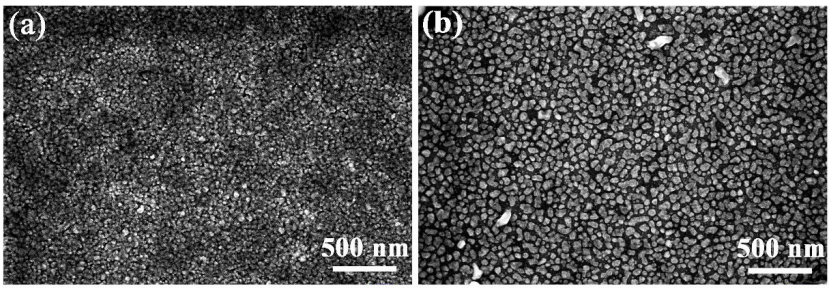

Figure 3. The SEM micrography of the NbTiAlSiNx nitride films after heat treatment at 1000 °C for 1 h. (**a**) N_2 = 4 sccm; and (**b**) N_2 = 8 sccm.

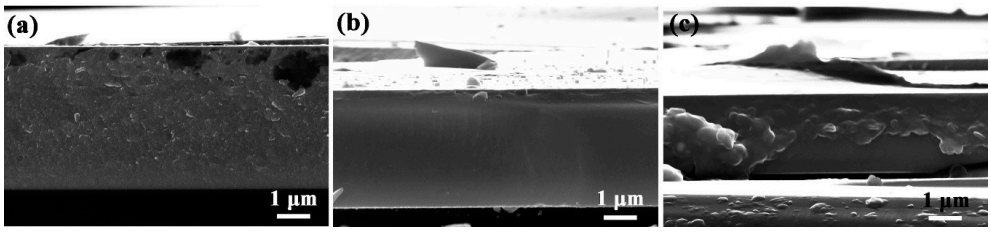

Figure 4. The SEM micrography of the $NbTiAlSiWN_x$ films after heat treatment at 1000 °C for 1 h. (**a**) N_2 = 0 sccm; (**b**) N_2 = 4 sccm; and (**c**) N_2 = 8 sccm.

Further research and development of the $NbTiAlSiWN_y$ films is still required. Compared to some other recently published high entropy films, the present films exhibit comparable advantages and promise as potential candidates for high temperature protective coatings. The results are summarized in Table 3.

Table 3. Comparison of recently reported film thermal stabilities.

Composition	Method	Duration (°C)	Holding Time	Reference
(TiVCrZrHf)N	sputtering	300	2 h in air	[23]
$Al_xCo_1Cr_1Cu_1Fe_1Ni_1$	sputtering	600	20 min vacuum	[24]
(AlBCrSiTi)N	sputtering	700	2 h vacuum	[25]
TaNbTiW	sputtering	700	90 min vacuum	[26]
6FeNiCoCrAlTiSi	laser cladding	750	5 h vacuum	[27]
$(NbTiAlSiW)N_x$	sputtering	700	24 h vacuum	this work

3.3. Mechanical Properties

The modulus of the as-deposited $NbTiAlSiN_y$ films decreases with the increase of N_2 flow and the hardness first increases from 18.1 GPa to a maximum value of 20.5 GPa (N_2 = 4 sccm), then decreases to 17.4 GPa. The load-depth, hardness, and modulus of the as-deposited $NbTiAlSiWN_y$ films are shown in Figure 5. It can be seen clearly that both modulus and hardness increase to maximum values of 13.6 GPa and 154.4 GPa (N_2 = 4 sccm) then decrease with increasing N_2 flow rate. This can be mainly attributed to the formation of saturated nitride and moderate grain size. The enhancement in hardness and modulus of nitride films are not significant. On the contrary, more nitride has a negative effect. The decrease in hardness results from more nitrogen making the film less dense and not as smooth as before. This phenomenon has been explained in our previous study.

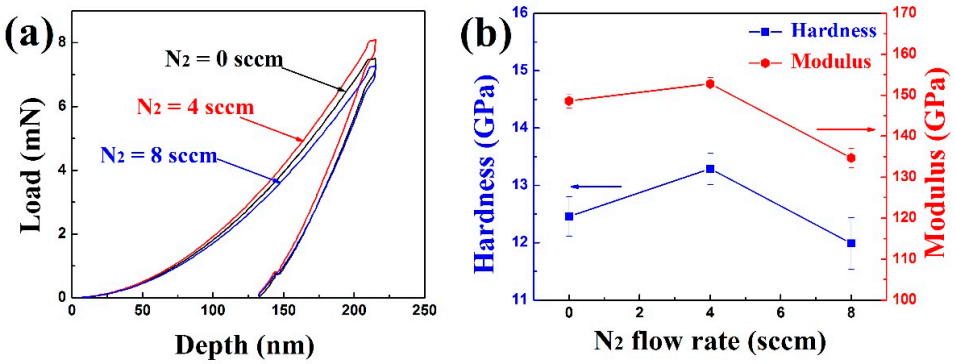

Figure 5. (**a**,**b**) Load-depth curves, hardness and modulus of the as-deposited $NbTiAlSiWN_x$ films with various N_2 flow rates, respectively.

4. Conclusions

The thermal stability and nanocrystalization process of $NbTiAlSiW_xN_y$ high-entropy films were discussed in the present work, and the conclusions are as follows: all the as-deposited films have amorphous structures, and near equimolar high-entropy NbTiAlSiW metallic films are achieved. Both the films exhibit excellent thermal stability, and can retain their amorphous structures even at 700 °C for 24 h. After heat treatment at 1000 °C for 1 h there was a change from an amorphous structure to a crystallized form with homogeneous nanoscaled grains. The hardness and modulus of the $NbTiAlSiWN_y$ films deposited under a N_2 flow of 4 sccm had a maximum hardness and modulus of 13.6 GPa and 154.4 GPa, respectively. This indicates that the $NbTiAlSiW_xN_y$ high-entropy films could be a good candidates as protective refined coatings.

Acknowledgments: The authors gratefully appreciate the financial supports from the National High Technology Research and Development Program of China (No. 2009AA03Z113), the National Science Foundation of China (No. 51471025).

Author Contributions: All authors have made contributions to this paper. Cong Wang and Yong Zhang conceived and designed the experiments; Wenjie Sheng and Xiao Yang performed the experiments and wrote the paper; Wenjie Sheng and Yong Zhang revised the paper. All authors discussed the results and reviewed the manuscript.

Conflicts of Interest: The authors declare no conflict of interest.

References

1. Yeh, J.W.; Chen, S.K.; Lin, S.J.; Gan, J.Y.; Chin, T.S.; Shun, T.T.; Tsau, C.H.; Chang, S.Y. Nanostructured high-entropy alloys with multiple principle elements: novel alloy design concepts and outcomes. *Adv. Eng. Mater.* **2004**, *6*, 299–303. [CrossRef]
2. Yeh, J.W.; Chen, S.K.; Gan, J.Y.; Lin, S.J.; Chin, T.S.; Shun, T.T.; Tsau, C.H.; Chang, S.Y. Formation of simple crystal structures in Cu-Co-Ni-Cr-Al-Fe-Ti-V alloys with multiprincipal metallic elements. *Metall. Mater. Trans. A* **2004**, *35A*, 2533–2536. [CrossRef]
3. Zhang, Y.; Zuo, T.T.; Tang, Z.; Gao, M.C.; Dahmen, K.A.; Liaw, P.K.; Lu, Z.P. Microstructures and properties of high-entropy alloys. *Prog. Mater. Sci.* **2014**, *61*, 1–93. [CrossRef]
4. Yeh, J.W. Recent progress in high entropy alloys. *Ann. Chim.* **2006**, *31*, 633–648.
5. Zhang, Y.; Qiao, J.W.; Liaw, P.K. A brief review of high entropy alloys and serration behavior and flow units. *J. Iron Steel Res. Int.* **2016**, *23*, 2–6. [CrossRef]
6. Li, J.M.; Yang, X.; Zhu, R.L.; Zhang, Y. Corrosion and serration behaviors of $TiZr_{0.5}NbCr_{0.5}V_xMo_y$ high entropy alloys in aqueous environments. *Metals* **2014**, *4*, 597–608. [CrossRef]
7. Chang, Z.C.; Liang, S.C.; Han, S.; Chen, Y.K.; Shieu, F.S. Characteristics of TiVCrAlZr multi-element nitride films prepared by reactive sputtering. *Nucl. Instrum. Methods Phys. Res. B* **2010**, *268*, 2504–2509. [CrossRef]
8. Liang, S.C.; Chang, Z.C.; Tsai, D.C.; Lin, Y.C.; Sung, H.S.; Deng, M.J.; Shieu, F.S. Structure and Mechanical Properties of Multi-element (TiVCrZrHf)N Coatings by Reactive Magnetron Sputtering. *Appl. Surf. Sci.* **2011**, *258*, 399–403. [CrossRef]
9. Tsai, D.C.; Chang, Z.C.; Kuo, B.H.; Chang, S.Y.; Shieu, F.S. Effects of silicon content on the structure and properties of (AlCrMoTaTi)N coatings by reactive magnetron sputtering. *J. Alloys Comp.* **2014**, *616*, 646–651. [CrossRef]
10. Liu, L.; Zhu, J.B.; Hou, C.; Li, J.C.; Jiang, Q. Dense and smooth amorphous films of multicomponent FeCoNiCuVZrAl high-entropy alloy deposited by direct current magnetron sputtering. *Mater. Des.* **2013**, *46*, 675–679. [CrossRef]
11. Ren, B.; Liu, Z.X.; Shi, L.; Cai, B.; Wang, M.X. Structure and properties of $(AlCrMnMoNiZrB_{0.1})N_x$ coatings prepared by reactive DC sputtering. *Appl. Surf. Sci.* **2011**, *257*, 7172–7178. [CrossRef]
12. Hu, Z.H.; Zhan, Y.Z.; Zhang, G.H.; She, J.; Li, C.H. Effect of rare earth Y addition on the microstructure and mechanical properties of high entropy AlCoCrCuNiTi alloys. *Mater. Des.* **2010**, *31*, 1599–1602. [CrossRef]
13. Hsu, C.Y.; Sheu, T.S.; Yeh, J.W.; Chen, S.K. Effect of iron content on wear behavior of $AlCoCrFe_xMo_{0.5}Ni$ high-entropy alloys. *Wear* **2010**, *268*, 653–659. [CrossRef]
14. Chen, Y.Y.; Duval, T.; Hung, U.D.; Yeh, J.W.; Shih, H.C. Microstructure and electrochemical properties of high entropy alloys—A comparison with type-304 stainless steel. *Corros. Sci.* **2005**, *47*, 2257–2279. [CrossRef]

15. Huang, C.; Zhang, Y.Z.; Shen, J.Y.; Vilar, R. Thermal stability and oxidation resistance of laser clad TiVCrAlSi high entropy alloy coatings on Ti–6Al–4V alloy. *Surf. Coat. Technol.* **2011**, *206*, 1389–1395. [CrossRef]
16. Tsai, M.H.; Wang, C.W.; Lai, C.H.; Yeh, J.W.; Gan, J.Y. Thermally stable amorphous $(AlMoNbSiTaTiVZr)_{50}N_{50}$nitride film as diffusion barrier in copper metallization. *Appl. Phys. Lett.* **2008**, *92*. [CrossRef]
17. Chang, S.Y.; Chen, D.S. Ultrathin $(AlCrTaTiZr)N_x$/AlCrTaTiZr Bilayer Structures with High Diffusion Resistance for Cu Interconnects. *J. Electrochem. Soc.* **2010**, *157*, G154–G159. [CrossRef]
18. Liang, S.C.; Tsai, D.C.; Chang, Z.C.; Lin, T.N.; Shiao, M.H.; Shieu, F.S. Thermally Stable TiVCrZrHf Nitride Films as Diffusion Barriers in Copper Metallization. *Electrochem. Solid State Lett.* **2012**, *15*, H5–H8. [CrossRef]
19. Tsai, M.H.; Yeh, J.W.; Gan, J.Y. Diffusion barrier properties of AlMoNbSiTaTiVZr high-entropy alloy layer between copper and silicon. *Thin Solid Films* **2008**, *516*, 5527–5530. [CrossRef]
20. Sheng, W.J.; Yang, X.; Zhu, J.; Wang, C.; Zhang, Y. Amorphous phase stability of $NbTiAlSiN_x$ high-entropy films. *Rare Metals* **2016**, accepted.
21. Guo, S.; Liu, C.T. Phase stability in high entropy alloys: Formation of solid-solution phase or amorphous phase. *Prog. Nat. Sci.* **2011**, *21*, 433–446. [CrossRef]
22. Klug, H.P.; Alexander, L.E. *X-Ray Diffraction Procedures for Polycrystalline and Amorphous Materials*; Wiley: New York, NY, USA, 1954.
23. Tsai, D.C.; Chang, Z.C.; Kuo, L.Y.; Lin, T.J.; Lin, T.N. Oxidation resistance and structural evolution of (TiVCrZrHf)N coatings. *Thin Solid Films* **2013**, *544*, 580–587. [CrossRef]
24. Wu, Z.F.; Wang, X.D.; Cao, Q.P.; Zhao, G.H.; Li, J.X.; Zhang, D.X.; Zhu, J.J.; Jiang, J.Z. Microstructure characterization of $Al_xCo_1Cr_1Cu_1Fe_1Ni_1$ (x = 0 and 2.5) high-entropy alloy films. *J. Alloys Comp.* **2014**, *609*, 137–142. [CrossRef]
25. Tsai, C.W.; Lai, S.W.; Cheng, K.H.; Tsai, M.H.; Davison, A.; Tsau, C.H.; Yeh, J.W. Strong amorphization of high-entropy AlBCrSiTi nitride film. *Thin Solid Films* **2012**, *520*, 2613–2618. [CrossRef]
26. Feng, X.G.; Tang, G.Z.; Gu, L.; Ma, X.X.; Sun, M.R.; Wang, L.Q. Preparation and characterization of TaNbTiW multi-element alloy films. *Appl. Surf. Sci.* **2012**, *261*, 447–453. [CrossRef]
27. Zhang, H.; Pan, Y.; He, Y.Z. Effects of Annealing on the Microstructure and Properties of 6FeNiCoCrAlTiSi High-Entropy Alloy Coating Prepared by Laser Cladding. *J. Thermal Spray Technol.* **2011**, *20*, 1049–1055. [CrossRef]